ELSEVIER

Journal of Orthopaedic Research 22 (2004) 1079–1085

Journal of Orthopaedic Research

www.elsevier.com/locate/orthres

Mechanical environment alters tissue formation patterns during fracture repair

E.A. Smith-Adaline [a], S.K. Volkman [a], M.A. Ignelzi Jr. [b], J. Slade [a], S. Platte [a], S.A. Goldstein [a,*]

[a] *Orthopaedic Research Laboratories, Department of Orthopaedic Surgery, University of Michigan, G-161 400 N. Ingalls, Ann Arbor, MI 48109-0486, USA*

[b] *Department of Orthodontics and Pediatric Dentistry, University of Michigan School of Dentistry, Ann Arbor, MI 48109, USA*

Received 14 May 2003; accepted 10 February 2004

Abstract

Fracture repair has previously been shown to be sensitive to mechanical environment, yet the specific relationship between strain character, magnitude and frequency, as well as other mechanical parameters, and tissue formation is not well understood. This study aimed to correlate strain distribution within the healing fracture gap with patterns of tissue formation using a rat model of a healing osteotomy subject to mechanical stimulation in bending. Finite element models based on realistic tissue distributions were used to estimate both the magnitude and spatial distribution of strains within the fracture gap. The spatial distribution of regenerating tissue was determined by microcomputed tomography and histology, and was confirmed using reverse transcription-polymerase chain reaction (RT-PCR). Results suggest that tensile strains suppress chondrogenesis during the mechanical stimulation period. After stimulation ends, however, tensile strains increased chondrogenesis followed by rapid bone formation. In contrast, in compressive environments, bone is formed primarily via intramembranous ossification. Taken together, these results suggest that intermittent tensile strains during fracture repair stimulate endochondral ossification and promote eventual bone healing compared to intermittent compressive strains and unstimulated fractures. Further understanding of these relationships may allow proposal of optimal therapeutic strategies for improvement of the fracture repair process.

Keywords: Fracture healing; Tissue differentiation; Mechanical loading; Finite element modeling

Introduction

Fracture healing is a complex process during which a cascade of gene expression drives the iterative formation and resorption of various tissues, eventually leading to bone formation that bridges the broken bone ends. The rate and efficacy of fracture repair depends on a variety of factors, including factors related to the patient (patient age); factors resulting from trauma (severity of trauma, fracture geometry and location); and factors operating during healing (nutritional status, hormonal milieu). In addition, mechanical environment has long been recognized to significantly influence the repair process. Several experimental studies have provided evidence that the mechanical environment may influence tissue differentiation during fracture healing. Mechanically manipulating the healing environment by altering fixation stiffness [10], axial dynamization [2], or applying controlled micromotions [9,11,19] has been shown to increase bone formation. In addition, studies on distraction osteogenesis have demonstrated that the extent of endochondral ossification and ultimately new bone formation depends on distraction rate and initial osteotomy geometry [15–18].

Despite these studies, the precise relationship between the local mechanical environment and patterns of bone repair is poorly understood. It is clear that theories regarding the response of bone repair to altered mechanical environments must be tested using animal models which allow controlled mechanical strains that can be either directly or indirectly estimated. This study aims to evaluate the association between the local mechanical strain environment and patterns of tissue

* Corresponding author. Tel.: +1-734-763-9674; fax: +1-617-647-0003/734-747-0003.

E-mail address: stevegld@umich.edu (S.A. Goldstein).

0736-0266/$ - see front matter © 2004 Orthopaedic Research Society. Published by Elsevier Ltd. All rights reserved.
doi:10.1016/j.orthres.2004.02.007

formation using a rat model of a healing osteotomy subjected to controlled mechanical stimulation in bending.

Materials and methods

Animal surgery and mechanical stimulation

A total of 70 male Sprague-Dawley rats underwent bilateral surgical procedures in which four 0.062″ diameter threaded pins were inserted percutaneously into the lateral aspect of both femora using a drill guide for placement. A custom unilateral external fixator containing a central hinge stabilized by a locking plate was then attached to the pins (Fig. 1). A 2 mm osteotomy was created in each leg through a small incision using an oscillating saw under constant saline irrigation, resulting in the removal of a small sliver of bone. Femora were radiographed post-operatively to ensure proper pin placement, and then weekly thereafter to monitor progression of healing.

One fracture in each animal was stimulated 3 times each week between 7 and 18 days post-operative (for a total of six loading sessions) using a custom stimulation device [19] under isoflurane anesthesia (see Fig. 1). During mechanical stimulation, fixators were attached to the stimulation device prior to removal of the locking plate. Activation of the device produces rotation of the fixator about its central hinge, which results in bending of the fracture gap tissue in the anterior–posterior direction. Fractures were mechanically stimulated for 17 min at 0.5 Hz, giving a total of 510 load cycles in each loading session ($17 \times 60 \times 0.5$ Hz $= 510$ cycles). Fixators were stabilized with a locking plate when not being stimulated to prevent motion around the hinge during normal cage activity. Contralateral fractures served as unstimulated controls. Animals were sacrificed at 7 ($n = 14$), 10 ($n = 8$), 14 ($n = 12$), 17 ($n = 7$), 21 ($n = 9$), 24 ($n = 4$), 28 ($n = 8$), or 42 ($n = 8$) days post-operative and both femora were harvested. Whole femora were removed from animals randomly assigned to one subset of 50 animals (referred to as subset A) sacrificed at 7 ($n = 10$), 10 ($n = 4$), 14 ($n = 9$), 17 ($n = 4$), 21 ($n = 7$), 28 ($n = 8$) and 42 ($n = 8$) days and were snap frozen. All pins and fixators were quickly removed after freezing, and femora were stored at −80 °C until further use. Fracture gap tissue was harvested from a separate subset of 20 animals (referred to as subset B) in the 7 ($n = 4$), 10 ($n = 4$), 14 ($n = 3$), 17 ($n = 3$), 21 ($n = 2$) and 24 ($n = 4$) day sacrifice groups under RNAse free conditions. Tissue was removed by two transverse cuts separating fracture gap tissue from cortical bone using a fresh scalpel blade. The tissue was immediately placed in RNALater (Ambion, Austin, TX) and stored at 4 °C.

Microcomputed tomography

All frozen femurs (subset A) were imaged using a microcomputed tomography (μCT) system [7] in a custom insulated fixture containing a liquid nitrogen chamber to maintain them in a frozen state. Images were reconstructed at a resolution of $50 \times 50 \times 50$ μm^3 and threshold values were determined for each image based on maximal grayscale value from image histograms. The analysis region in the axial direction was defined by fitting a plane to a set of eight (x, y, z) coordinates that defined the proximal and distal cut bone ends. Lateral borders of the analysis region were chosen as the outermost border of the callus. Contiguity of bone between the osteotomized bone ends was calculated for each point on the (x, y) plane (transverse) as the number of bone voxels in the z-direction divided by the total number of voxels in that column. Bone volume fraction (BV/TV) in the fracture gap was cal-

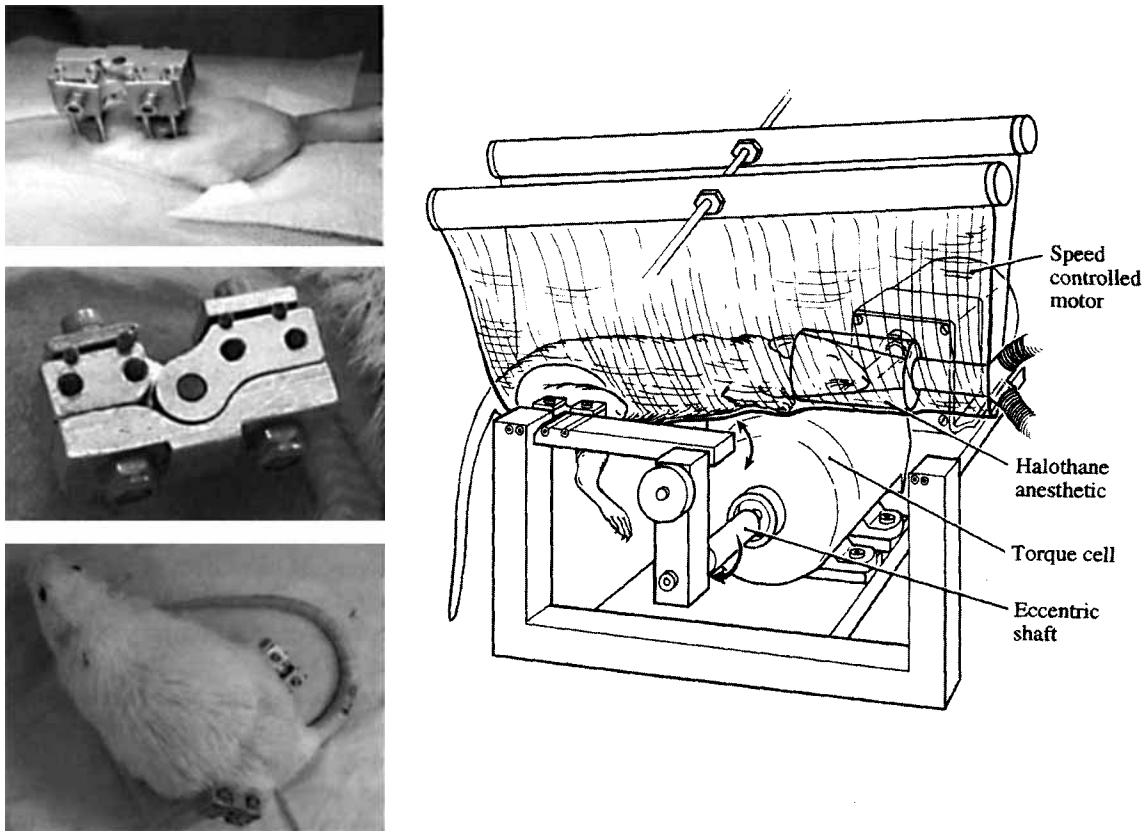

Fig. 1. The external fixator is illustrated demonstrating the placement on the femur and the included hinge and locking plate. A schematic drawing of rat positioned in mechanical loading device with external fixator attached to device. Rotational displacement is driven by a rotary motor attached to an eccentric cam. Two rigid linkages are used to attach the cam to the fixator. The rotational motion then produces bending of the fixator at the central hinge.

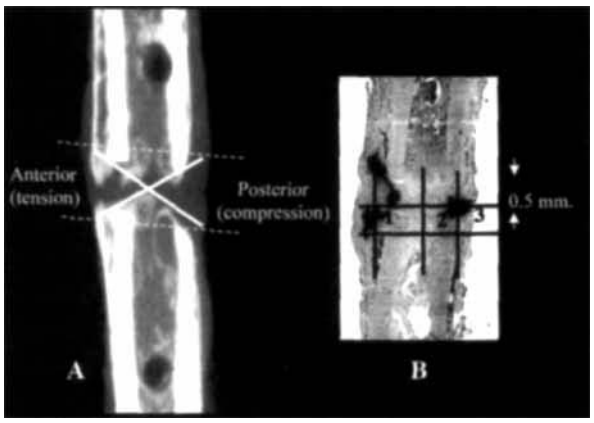

Fig. 2. (A) The data from MicroCT was segmented by drawing two diagnols from the outer edges of the cut bone cortices. These defined the posterior and anterior quadrants. (B) For histologic analysis, the fracture gap tissue was divided into three regions for analysis.

culated by dividing the number of voxels that were above the bone threshold value (BV) by the total number of voxels in the analysis region (TV). Contiguity and BV/TV were assessed in the entire fracture gap, as well as in quadrants defined by intersecting diagonal lines drawn from opposite corners of the analysis region. These quadrants distinguished regions of the fracture gap that were primarily exposed to tension (anterior) or compression (posterior) (see Fig. 2).

Histology and stereology

A small group of frozen femurs from subset A were fitted with a temporary fixator, and were thawed and fixed in 4% paraformaldehyde. These specimens were from the 7 ($n = 3$), 10 ($n = 3$), 14 ($n = 5$), 17 ($n = 4$), 21 ($n = 4$), 28 ($n = 4$) and 42 ($n = 4$) day time points. Femora were decalcified in formic acid buffered with sodium citrate and embedded in paraffin before removal of the stabilizing fixators. Two 7 μm-thick mid-sagittal sections from each specimen were stained with 0.02% fast green and 1.0% safranin-O. Cartilage area fraction (CA/TA) was measured as the area stained with safranin-O (CA) divided by the total analysis area (TA) using digital microscope images from each section using BioQuant NOVA software (R&M Biometrics, Nashville, TN). Analysis was performed in the central 0.5 mm of the fracture gap, which was divided into three regions representing regions primarily exposed to tension, neutral, or primarily under compression during mechanical loading (see Fig. 2).

RNA extraction and reverse transcription-polymerase chain reaction (RT-PCR)

Gene expression within the entire fracture gap was assessed using RT-PCR. Fracture gap tissue was homogenized both mechanically using a tissue homogenizer and enzymatically using Trizol (Gibco BRL, Grand Island, NY) under RNAse-free conditions. Total RNA was isolated, and expression of type II collagen and GAPDH was analyzed using RT-PCR. Briefly, a 0.5 μg aliquot of RNA from each sample was reverse transcribed using the GeneAmp system (Perkin–Elmer, Wellesley, MA), and a 2 μl aliquot of cDNA template was used for PCR amplification of type II collagen or GAPDH. Type II collagen was amplified using primers 5′-TTGGTGTGGACATAGGGCCT-3′ and 5′-GTCTGCCCAGTTCAGGTCTC-3′ [1] and the PCR reaction was carried out for 25 cycles of at an annealing temperature of 60 °C. GAPDH was amplified using primers 5′-ACCCATCACCATCTTC-CAGGAGCGC-3′ and 5′-AGGCCATGCCAGTGAGCTTCCCG-3′ and the PCR reaction was carried out for 18 cycles at an annealing temperature of 55 °C [6]. Semi-quantitative analysis of type II collagen PCR products was performed densitometrically on digital images (Kodak Digital Science Electrophoresis Documentation and Analysis System 120, New Haven, CT) using the NIH Image gel-plotting macro (Bethesda, MD). Detection of GAPDH PCR products was performed using a digoxygenin-labeled PCR ELISA technique (Roche Molecular Biochemicals, Indianapolis, IN). The band intensity of type II collagen PCR products was then normalized to GAPDH expression.

Finite element modeling

Finite element models were created for two representative specimens sacrificed at 7 and 14 days post-operative, which correspond to the beginning of each week of mechanical stimulation. The goal of mesh generation was to realistically represent the spatial distribution of resident tissues, specifically bone, cartilage, and undifferentiated connective tissue. Bone elements were obtained from microcomputed tomography images of the entire femur, which were directly converted into a finite element mesh by converting each voxel into an 8-noded hexagonal element. Spatial distribution of cartilage was determined qualitatively for each specimen using histological sections taken though the entire fracture gap, and appropriate cartilage elements were added to the model manually using Hypermesh software (Altair Engineering, Troy, MI). The remaining elements contained within the fracture gap region were considered to be connective tissue. Models generally contained approximately 200,000–250,000 elements. Boundary conditions were applied to mimic the motion of the fixator during mechanical stimulation. The angle of rotation of the central hinge of the fixator was determined to be 1.61°, which resulted in a translation of approximately 0.155 mm at the center of the inner distal pin. The proximal pin track was constrained in all 6 degrees of freedom. Progressive translations towards the posterior surface (in the x-direction) were applied to the distal pin tract to create bending, while displacement in the y- (medial–lateral) and z- (axial) directions were constrained. Material properties were assigned to cortical bone ($E = 18,668$ MPa; $\nu = 0.30$ [14]), cartilage ($E = 15$ MPa, $\nu = 0.47$ [8]) and connective tissue ($E = 3.0$ MPa, $\nu = 0.40$ [5]) elements based on reported values. Models were analyzed using an element-by-element preconditioned conjugate gradient technique with a convergence tolerance of 1.0×10^{-4}. Stresses and strains were recovered for each element, and averages were calculated for the entire model as well as in element subsets defining regions that are primarily exposed to tensile, neutral, and compressive strains.

Statistical analysis

Differences in BV/TV between loaded and control specimens at each time point were determined using a Wilcoxin signed rank test. Regional differences in average contiguity and CA/TA between loaded and control specimens at each time point were also analyzed using a Wilcoxin signed rank test. For all analyses, the attained p values were calculated.

Results

Finite element analyses for both the 7- and 14-day models demonstrated a consistent strain gradient in the axial direction (z-direction). In general, the anterior cortex experienced high tensile strains and the posterior cortex experiences high compressive strains (see Fig. 3), while strains in the medial–lateral direction (y-direction) remain constant (data not shown). Average strains in the tensile (anterior) zone range from +1.7% to +2.4% and strains in the compressive (posterior) zone range from −0.98% to −2.2%. Maximum strains are approximately three times greater than average strains in each region. Therefore, finite element analyses predict that the total strain gradient resulting from bending stimulation is approximately 7% strain in tension to 3.5% strain in compression, with very little variation between the 7- and 14-day models.

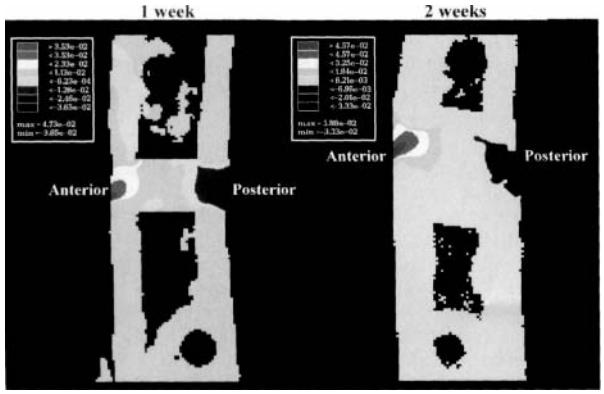

Fig. 3. Typical strain distributions of one and two week finite element models. Both images demonstrate high tensile strains on the anterior cortex (left) and high compressive strains on the posterior cortex (right).

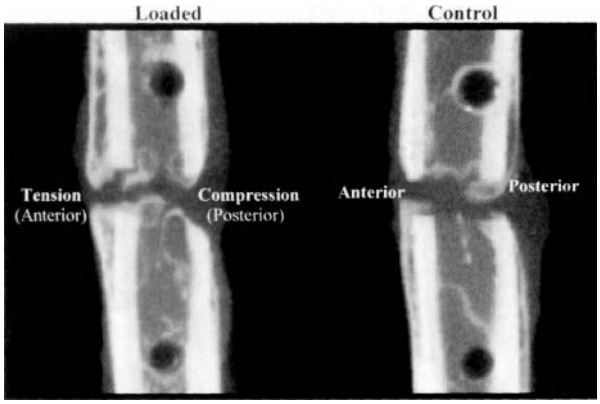

Fig. 4. MicroCT images of loaded and contralateral control fractures from one animal at 42 days post-operative. The loaded specimen exhibits distinct patterns of osteogenesis in the area experiencing primarily tensile strains, while the control specimen shows no clear pattern of bone formation.

Microcomputed tomography (μCT) images from long-term (42 days) animals show substantial bone formation in the region that experienced tension, while bone formation seems to be suppressed in areas of compression (see Fig. 4). While these images from planes of data (50 μm thick) provide a global view of the healing patterns, the volume fraction and continuity measures provide a method to quantify regions of boney bridging that occur throughout the three-dimensional structure. Quantitative analysis of bone formation in the entire gap (shown in Table 1) demonstrated trend towards decreased BV/TV at the end of the stimulation period (i.e. at 21 days post-operative) ($p = 0.13$). Analysis of average contiguity in the tensile quadrant showed a trend towards decreased contiguity in loaded fractures until 42 days post-operative, at which time contiguity tended to exceed controls ($p = 0.12$). Closer examination indicated that tensile regions of loaded fractures demonstrated an increase in average contiguity at 42 days post-operative partly because of a trend towards an increased percentage of the quadrant that is completely bridged (i.e. 100% contiguous) compared to compressive regions. In contrast, no differences in average or long-term contiguity between loaded and control fractures were evident in the posterior (compressive) quadrant.

Cartilage area fraction results demonstrate that cartilage formation is inhibited in tensile regions of loaded compared to control specimens. This is particularly evident during the mechanical stimulation period (up to 21 days) (see Fig. 5). After the mechanical stimulation period ended, cartilage area fraction rapidly increased between 21 and 28 days in tensile regions of loaded specimens. By 42 days post-operative, the amount of cartilage in tensile regions of loaded specimens is drastically decreased ($p = 0.068$), while cartilage persists in unstimulated specimens. Chondrogenesis appears to be suppressed in the neutral and compressive regions during the stimulation period, but is indistinguishable from controls at longer time points (28 and 42 days). These results are consistent with RT-PCR analysis of type II collagen expression. A general trend towards decreased type II collagen expression in loaded fractures is apparent during the stimulation period (i.e. 14 and 17 days), although these data did not reach statistical significant. In contrast, at later time points type II collagen expression decreases more rapidly in loaded fractures than controls (see Fig. 6).

Table 1
Measures of bone formation

Time (days)	BV/TV		Average contiguity (anterior)		Average contiguity (posterior)	
	Loaded	Control	Loaded	Control	Loaded	Control
7	–	0.0282 ± 0.0118	–	0.0233 ± 0.0153	–	0.0233 ± 0.0192
10	0.0256 ± 0.0060	0.0303 ± 0.0069	0.0223 ± 0.0106	0.0319 ± 0.0040	0.0257 ± 0.0047	0.0209 ± 0.0085
14	0.0447 ± 0.0270	0.0490 ± 0.0398	0.0390 ± 0.0196	0.0611 ± 0.0644	0.0705 ± 0.0712	0.0397 ± 0.0221
17	0.0600 ± 0.0381	0.0539 ± 0.0200	0.0639 ± 0.0749	0.0437 ± 0.0218	0.0576 ± 0.0181	0.0562 ± 0.0238
21	0.1173 ± 0.0496[a]	0.1484 ± 0.0882	0.1107 ± 0.0675	0.1341 ± 0.0969	0.1071 ± 0.0520[a]	0.1691 ± 0.0865
28	0.1858 ± 0.0715	0.2486 ± 0.0090	0.1861 ± 0.1615	0.2654 ± 0.1113	0.1996 ± 0.1093	0.2169 ± 0.0799
42	0.4167 ± 0.1744	0.4256 ± 0.1510	0.4576 ± 0.2299[a]	0.3628 ± 0.1739	0.3676 ± 0.1859	0.3917 ± 0.1584

All values presented as mean ± standard deviation.
[a] $p = 0.13$ vs. control.

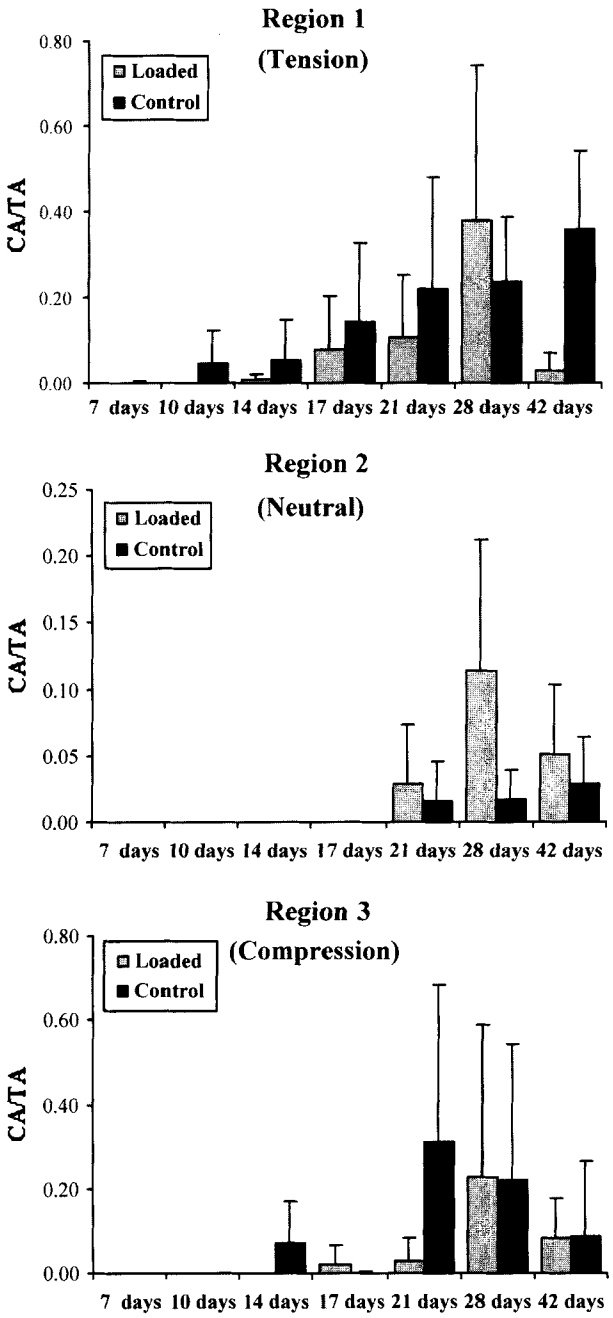

Fig. 5. Graphs depicting distribution of cartilage in tensile, neutral and compressive regions at various time points post-operative. The loaded fractures are represented by the light color while the control data is represented by the dark bars. Cartilage appears to be limited to tensile regions during the stimulation period (between 7 and 21 days). Cartilage apparent in tensile region disappears after stimulation ended, between 28 and 42 days, suggesting that this region undergoes rapid endochondral ossification.

Discussion

The goal of this study was to correlate the mechanical strain environment created by mechanical stimulation of a fracture with patterns of tissue regeneration during bone repair. Finite element models predicted the strain

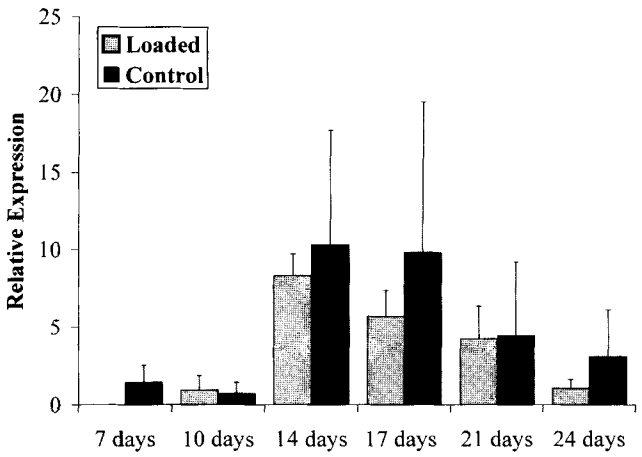

Fig. 6. Expression of type II collagen normalized to GAPDH as determined by PCR for the entire fracture repair tissue. The dark shaded bars represent the control tissue while the light colored bars depict the data for the loaded tissues. By 24 days, the results support the observation of a tendency for decreased cartilage production (data are expressed as a percent of GAPDH density).

environment generated by the bending stimulus to range from 7% in tension to 3.5% in compression. These computational models were based on realistic geometry obtained from high-resolution μCT images and histological sections, and realistic boundary conditions resulting from the imposed bending stimulus. This approach poses distinct advantages over previously reported attempts to model the mechanical environment during bone regeneration. First, the mechanical stimulation protocol results in application of a well-controlled mechanical stimulus in terms of strain magnitude and frequency to the repair tissue. Because the boundary conditions during stimulation are well defined, reasonable estimates of the local strain environment within the fracture gap can be obtained, which can then be directly compared to experimental results. Second, the analysis is based on realistic geometry of the fracture gap and the surrounding cortical bone since the finite element mesh is created from digital μCT images. In contrast, many previous studies have been limited to two-dimensional analyses with idealized geometry and boundary conditions.

Differences in the dynamics of chondrogenesis and osteogenesis were found between regions experiencing tensile and compressive strains, and between stimulated and unstimulated control fractures. Bone formation seemed to be unaffected in loaded fractures during the stimulation period, yet at longer time points (i.e. 42 days post-operative) the extent of bone bridging the fracture gap tended to be increased only in tensile regions of stimulated fractures. Since osteogenesis is not obviously altered during the two-week period of mechanical stimulation, the effect of strain environment on bone formation must be secondary to other cellular or molecular processes that are directly influenced by stimulation.

Cartilage formation, however, did appear to be inhibited by mechanical stimulation during the stimulation period in areas experiencing either tensile or compressive strains. As early as one week after stimulation ends, loaded specimens exhibited a robust chondrogenic response, and the cartilage area fraction in tensile regions tended to exceed that of control samples. Then, the amount of cartilage in tensile regions is drastically reduced by 42 days post-operative, which implies that this cartilage has rapidly undergone endochondral ossification.

Chondrogenesis increased dramatically in tensile regions immediately after the cessation of mechanical stimulation, and subsequently cartilage was rapidly replaced by bone. It is hypothesized that this could result an early increase in proliferation of progenitor cells stimulated by tensile mechanical signals, combined with an inhibition of differentiation into chondrogenic and/or osteogenic cells. Such an increase in the population of mesenchymal progenitor cells could account for both the rapid chondrogenic and osteogenic responses observed after mechanical stimulation ended. This hypothesis is consistent with previous results in the literature. Turner [21] demonstrated that mechanical loading of intact rat tibiae resulted in increased proliferation of osteoprogenitor cells as well as increased progenitor cell differentiation into osteoblasts. In addition, skeletal unloading has been shown to decrease proliferation of osteoprogenitor cells [12] as well as their sensitivity to growth factor stimulation [13]. This suggests that the effects seen in this model could result either from direct stimulation of osteoprogenitor cells or indirectly via production or responsiveness to mitogenic or differentiation factors.

Compressive strains did not appear to dramatically alter the long-term outcome of the repair process, since no differences between loaded and control fractures were apparent in BV/TV of compressive zones at 42 days. However, compressive regions exhibit approximately a 40% decrease in the maximum cartilage area fraction when compared to tensile regions, yet only about a 20% decrease in the amount of bone present at long time points. This suggests that the proportion of bone being formed by an intramembranous or direct pathway may be increased in compressive regions. These results do not agree with previous theories regarding mechanical influences on tissue formation. While Roux predicted that compressive strains induce bone formation, which is consistent with these results, Roux further assumed that tensile strains favored connective tissue formation [20]. Results from this study suggest that tension promotes endochondral ossification. The results seen during the stimulation period may also contradict some aspects of the interfragmentary strain hypothesis (IFSH) proposed by Perren [17]. Perren's theory suggests that increased interfragmentary strain within the healing fracture gap would stimulate production of an intermediate tissue, such as cartilage, as long as strain magnitudes are below the failure strain of cartilage. This serves to add rigidity to the gap tissue and reduce strain until it is below failure strain of bone, therefore at an acceptable level for bone formation. Therefore, this hypothesis would predict an increase in cartilage production as a direct result of an applied mechanical stimulation, particularly since strain levels in this model were substantially less than the failure strain of cartilage (i.e. about 20% strain [17]). The results of this study, however, suggest that chondrogenesis is inhibited during the stimulation period. In contrast, results from time points beyond the stimulation period agree with the IFSH. By 6 weeks, it appears that high tensile strains resulted in increased bone formed by endochondral ossification compared to both unstimulated fractures and compressive strain regions.

Carter et al. [4] and Blenman et al. [3] theorized that high stress magnitudes induce tissue proliferation, while low stress magnitudes result in osteogenesis; shear and/or tensile hydrostatic strains favor fibrous tissue formation; and high compressive hydrostatic strains promote formation of cartilage. This theory agrees with the results of the current study in terms of strain magnitude, in which higher magnitudes of tensile strains resulted in cellular proliferation, while smaller magnitudes of compressive strains may encourage intramembranous ossification. However, the predictions of this theory based on strain character (i.e. tensile or compressive strains) are not consistent with these results. It is important to appreciate, though, that these theories are based on simplifications of strain environment, where strains are considered to be static, uniaxial, and homogeneous. In reality, the healing tissue in this study are subjected to cyclic loading, in which the strain state is not only three-dimensional, but is also constantly changing, including time-dependent effects due to the viscoelastic nature of soft biological tissues. Therefore, it is unlikely that these simple theories could realistically predict tissue differentiation in response to a complex strain environment.

Results of this study are subject to several limitations. First, finite element analyses assumed that the resident tissues of the fracture gap were linearly elastic and homogeneous. In addition, only one loading cycle was modeled, neglecting the time-dependent response of soft biological tissues. Analyses of bone volumes involved assumptions about the geometry of the tissue. For example, BV/TV and contiguity were calculated over a rectangular region defined by the outer edge of the callus, while the callus is generally rounded at its outer edge. Therefore, "dead spaces" in the analysis region were probably included in calculations of total volume. In addition, data did not reach clear statistical significance in these analyses, which was likely due in part to

the small sample sizes in each group. Because of this, further studies in this area may be necessary to verify the interesting trends suggesting a meaningful osteogenic and chondrogenic response to the mechanical environment. Despite these limitations, results from this study suggest that a controlled mechanical stimulus alters patterns of tissue formation. Tensile strains tended to promote endochondral ossification, hypothetically by increasing the pool of mesenchymal progenitor cells, and by 42 days demonstrated a general increase in bony bridging. In contrast, compressive strains appear to suppress chondrogenesis and favor direct intramembranous bone formation. Overall, these data suggest that alterations in the local mechanical environment during fracture healing may alter the phenotypic behavior of the healing tissues and may be a strategic target for therapeutic intervention.

Acknowledgements

Financial support for this research was provided by NIH DE 13014 and training grant NIA T32 AG00114 (ESA). The authors wish to thank Mitchell Schaffler for valuable input into this research program, and Scott Hollister for advice on finite element modeling and for analysis code. In addition, we wish to acknowledge Jan Hall, Kathy Sweet, Bonnie Nolan, Kelly Lucas, Dennis Kayner, Mark Stock, Charles Roehm, John Baker, Rochelle Taylor, Ryan Stayton, Meredith Duran, Jennifer Dreier, Azi Yavari and Wei Wang for their contributions to this study.

References

[1] Alvarez J, Balbin M, Fernandez M, Lopez JM. Collagen metabolism is markedly altered in the hypertrophic cartilage of growth plates from rats with growth impairment secondary to chronic renal failure. J Bone Mineral Res 2001;16:511–24.

[2] Aro HT, Chao EY. Bone-healing patterns affected by loading, fracture fragment stability, fracture type, and fracture site compression. Clin Orthop Relat Res 1993:8–17.

[3] Blenman PR, Carter DR, Beaupre GS. Role of mechanical loading in the progressive ossification of a fracture callus. J Orthop Res 1989;7:398–407.

[4] Carter D, Blenman P, Beaupre B. Correlations between mechanical stress history and tissue differentiation in initial fracture healing. J Orthop Res 1988;6:736–48.

[5] Claes LE, Heigele CA. Magnitudes of local stress and strain along bony surfaces predict the course and type of fracture healing. J Biomech 1999;32:255–66.

[6] Dusterhoft S, Putman CT, Pette D. Changes in FGF and FGF receptor expression in low-frequency-stimulated rat muscles and rat satellite cell cultures. Differentiation 1999;65:203–8.

[7] Feldkamp LA, Goldstein SA, Parfitt AM, et al. The direct examination of three-dimensional bone architecture *in vitro* by computed tomography. J Bone Mineral Res 1989;4:3–11.

[8] Fujii T, Takai S, Arai Y, et al. Microstructural properties of the distal growth plate of the rabbit radius and ulna: biomechanical, biochemical and morphological studies. J Orthop Res 2000;18:87–93.

[9] Goodship AE, Kenwright J. The influence of induced micromovement upon the healing of experimental tibial fractures. J Bone Joint Surg—British Vol 1985;67:650–5.

[10] Goodship AE, Watkins PE, Rigby HS, Kenwright J. The role of fixator frame stiffness in the control of fracture healing. An experimental study. J Biomech 1993;26:1027–35.

[11] Kershaw CJ, Cunningham JL, Kenwright J. Tibial external fixation, weight bearing, and fracture movement. Clin Orthop Relat Res 1993:28–36.

[12] Kostenuik PJ, Halloran BP, Morey-Holton ER, Bikle DD. Skeletal unloading inhibits the *in vitro* proliferation and differentiation of rat osteoprogenitor cells. Am J Physiol 1997;273: E1133–9.

[13] Kostenuik PJ, Harris J, Halloran BP, et al. Skeletal unloading causes resistance of osteoprogenitor cells to parathyroid hormone and to insulin-like growth factor-I. J Bone Mineral Res 1999;14: 21–31.

[14] Lee FY, Rho JY, Harten Jr R, Parsons JR, Behrens FF. Micromechanical properties of the epiphyseal trabecular bone and primary spongiosa around the physis an in situ nanoindentation study. J Pediatr Orthop 1998;18:582–5.

[15] Li G, Simpson AH, Kenwright J, Triffitt JT. Assessment of cell proliferation in regenerating bone during distraction at different distraction rates. J Orthop Res 1997;15:765–72.

[16] Li G, Simpson AHRW, Kenwright J, Triffitt JT. Effect of lengthening rate on angiogenesis during distraction osteogenesis. J Orthop Res 1999;17:362–7.

[17] Perren SM. Physical and biological aspects of fracture healing with special reference to internal fixation. Clin Orthop Relat Res 1979:175–96.

[18] Richards M, Kozloff KM, Goulet JA, Goldstein SA. Increased distraction rates influence precursor tissue composition without affecting bone regeneration. J Bone Mineral Res 2000;15: 982–9.

[19] Rouleau JP. Influence of strain amplitude and stimulation timing on secondary fracture healing. Ann Arbor, MI, PhD thesis, University of Michigan, 1996.

[20] Roux W. Gessamelte abhandlungen uber entwicklungsmechanik der organismen. Leipzig: Willhelm Engelmann; 1895.

[21] Turner CH. Recruitment and proliferative responses of osteoblasts after mechanical loading *in vivo* determined using sustained-released bromodeoxyuridine. Bone 1998;22:463–9.